

## Dynamical and thermodynamical instabilities in the disordered $\text{Re}_x\text{W}_{1-x}$ system

Kristin Persson, Mathias Ekman, and Göran Grimvall

*Theoretical Physics, Department of Physics, Royal Institute of Technology, SE-100 44 Stockholm, Sweden*

(Received 22 December 1998; revised manuscript received 12 May 1999)

The dynamical and thermodynamical stability of the bcc and fcc disordered  $\text{Re}_x\text{W}_{1-x}$  system is studied within the density-functional theory. The configurational part of the free energy is obtained from *ab initio* electron structure calculations together with the cluster expansion and the cluster variation formalism. Electronic excitations are accounted for through the temperature-dependent Fermi-Dirac distribution. The lattice dynamics of Re and W is studied using the density-functional linear-response theory. The calculated dispersion curves show that fcc Re is dynamically stable while bcc Re exhibits phonon instabilities in large parts of the Brillouin zone, similar to previous results for fcc W. Interestingly, the phonon dispersion curves for fcc Re show pronounced phonon anomalies characteristic of superconductors such as TaC and NbC. Due to the instabilities in bcc Re and fcc W the vibrational entropy, and therefore the free energy, is undefined. In order to predict the regions where the disordered  $\text{Re}_x\text{W}_{1-x}$  alloy is unstable we calculate the phonon dispersion curves in the virtual crystal approximation. Then we apply a concentration-dependent nonlinear interpolation to the force constants, which are calculated through a Born-von Kármán fit to the *ab initio* obtained dynamical matrices. The vibrational free energy is calculated in the stable regions for the phases as a function of concentration. The complete analysis gives a region where the bcc phase would become thermodynamically unstable towards a phase decomposition into disordered bcc and fcc phases. [S0163-1829(99)11537-6]

### I. INTRODUCTION

Alloys of the group-VI metals Cr, Mo, and W with Re have been studied extensively in experiments.<sup>1-5</sup> One reason is that a small addition of Re to these elements simultaneously increases their strength and plasticity. This so-called rhenium effect has since then become a collective name for the numerous changes in the group-VI metal properties due to small additions of Re. Rhenium-molybdenum alloys in the  $\sigma$  phase and the A15 structure as well as the Re-W hcp alloy system have been studied because of their superconducting properties.<sup>6-8</sup>

Tungsten has been suggested as armor material in plasma facing components in future fusion devices. This has increased the interest in the Re-W system because the heavy neutron irradiation from the fusion process transforms W atoms into Re. After many years of service the Re concentration in the bulk may be as high as 25%, which is close to the solubility limit of the bcc W-Re solid solution.<sup>9</sup> However, in the case of irradiation the Re atoms are created randomly on the bcc lattice, which means that higher Re concentrations can be reached than what corresponds to the phase diagram of thermal equilibrium. It has been observed<sup>1</sup> that the elastic constant  $C'$  in W decreases with Re alloying, which is a sign of growing instability of the bcc crystal.

There is not much theoretical work on W-Re alloys.<sup>10,11</sup> In particular, no attention has yet been given to the stability of the bcc Re-W system when the Re concentration of an irradiated sample exceeds the solubility limit. We therefore perform an *ab initio* study of the dynamical and thermodynamical stability of bcc Re and the disordered bcc Re-W system. The stable phase of pure Re has the hcp lattice structure. However, our main concern is the bcc phase, but we need a stable Re reference structure and choose fcc Re. The fcc phase is also a candidate for the metastable phase ob-

served in undercooled Re.<sup>12</sup> The study of the Re-W alloys will also present an interesting example of how to deal with the free energy in systems with thermodynamically stable and metastable, as well as dynamically unstable, phases. There are advantages in choosing Re and W. The masses are almost equal, which greatly facilitates the calculation of the phonon frequencies in the disordered case. Also, the relaxation effects are reduced due to the small size mismatch which gives us a clearer picture of the other contributions to the free energy. The purpose of the paper is therefore two-fold: (i) to perform *ab initio* electron structure calculations on a particular system of importance in possible applications and for which there are no previous calculations, and (ii) to illustrate the effect of lattice instabilities in the phase diagram of an alloy at finite temperatures.

This paper is organized as follows. In Sec. II, the formalism of cluster expansion, the derivation of the free energy, and the details of our calculations are given. Section III presents the dynamical stability based on the phonon dispersion curves for the ordered bcc and fcc phases and the thermodynamical stability of the disordered bcc and fcc phases. A summary is given in Sec. IV.

### II. FORMALISM

#### A. Cluster expansion of the total energy

A well established method for treating substitutional (dis)order in an  $A_xB_{1-x}$  alloy system is to map the alloy problem to an Ising model, where the different ions are assigned to the sites of the Ising lattice. The mapping can be described by a site occupation operator  $\sigma_i$ , which takes the value  $-1(+1)$  if the lattice site  $i$  is occupied by an A (B) atom. Let the Ising lattice ( $L$ ) have  $N$  sites. Any configuration can then be specified by a  $N$ -dimensional vector  $\sigma = (\sigma_1, \dots, \sigma_N)$ . In the seminal paper of Sanchez, Ducastelle,

and Gratiás<sup>13</sup> it was shown that any given function of the configuration can be expanded in a set of functions that depends on the configuration.

For each cluster  $\alpha \equiv (p_1, p_2, \dots, p_{n_\alpha})$ , containing  $n_\alpha$  lattice sites, we define a complete set of orthogonal cluster functions  $\Phi_\alpha$  as

$$\Phi_\alpha(\sigma_{p_1}, \dots, \sigma_{p_{n_\alpha}}) = \sigma_{p_1} \sigma_{p_2} \cdots \sigma_{p_{n_\alpha}}. \quad (1)$$

Every configuration-dependent property can now be expanded in this basis. For the total energy we get

$$E(\sigma) = \sum_{\alpha} V_{\alpha} \Phi_{\alpha}(\sigma), \quad (2)$$

where  $V_{\alpha}$  are referred to as the *effective cluster interactions* (ECI's), and Eq. (2) is the *cluster expansion* (CE) of the total energy. The expression in Eq. (2) is exact if we include all  $2^N$  terms. The work required to determine all ECI's is of the same order as determining the total energy of all  $2^N$  configurations.

The usefulness of this theory resides in the fact that only a small set of clusters is needed for the series to converge reasonably well. One introduces a largest cluster,  $\alpha_M$ , beyond which interactions are ignored. In the structural inversion method<sup>14</sup> (SIM) the ECI's are used as a set of fitting parameters. The ECI's are obtained by fitting the truncated form of Eq. (2) to a set of *ab initio* calculated energies for some ordered structures  $\{\phi\}$ . The linear dependence of the total energy on the configuration is thus obtained from a rather small number of total-energy calculations which can be performed by a state-of-the-art density functional method.

The expansion coefficients in Eq. (2) possess the symmetry of the underlying Ising lattice  $L$ .<sup>15</sup> Thus, all clusters that are equivalent by some lattice symmetry operation have equal ECI's. Such a set of ECI's is said to be in the same *orbit*,  $\Omega_L(\alpha)$ . It is necessary to take this into account when obtaining the ECI's. Using the symmetry argument we can rewrite Eq. (2) by grouping equivalent terms together as

$$\varepsilon(\sigma) = \frac{E(\sigma)}{N} = \sum_{\Omega_L(\alpha)}^{N_{\text{ECI}}} V_{\alpha} m_{\alpha} \Phi_{\alpha}(\sigma), \quad (3)$$

$$\Phi_{\alpha}(\sigma) \equiv \frac{1}{N_{\alpha}} \sum_{\beta \in \Omega_L(\alpha)}^{N_{\alpha}} \Phi_{\beta}(\sigma), \quad (4)$$

where the  $m_{\alpha}$  is the number of  $\alpha$  clusters per lattice site. Using Eq. (3) for the site energy in the SIM, we have to minimize the following weighted variance:

$$w = \sum_{\{\phi\}}^Z \omega_{\phi} \left[ \varepsilon(\phi) - \sum_{\Omega_L(\alpha)}^{N_{\text{ECI}}} m_{\alpha} V_{\alpha} \Phi_{\alpha}(\phi) \right]^2, \quad (5)$$

where  $N_{\text{ECI}}$  is the number of  $V_{\alpha}$  to be determined. In this paper  $\omega_{\phi} = 1$  is used, but other choices exist.<sup>16</sup>

### B. The configurational part of the energy

The CE is an expansion of the configurational dependence, i.e., the energies used as input in the SIM should ‘‘only’’ have this dependence. This is not the case for the measured enthalpies of formation, because in addition they

contain elastic contributions due to different equilibrium volumes. The enthalpy of formation  $\Delta H(\sigma)$  is defined as

$$\Delta H(\sigma) = \Delta E(\sigma, V_{\sigma}) = \min_V \Delta E(\sigma, V), \quad (6)$$

where

$$\Delta E(\sigma, V) = E(\sigma, V) - x E_A - (1-x) E_B. \quad (7)$$

$E(\sigma, V)$  is the energy of the compound,  $x$  the concentration of constituent  $A$  and  $E_A$  ( $E_B$ ) is the energy of  $A$  ( $B$ ) at its equilibrium volume  $V_A$  ( $V_B$ ). If one uses this set of energies in the SIM, then the volume independence would propagate through the CE, leading to an alloy with vanishing bulk modulus. However, an approximate<sup>17</sup> way of dealing with the volume dependence in the CE is to use totally relaxed energies, i.e., enthalpies of formation  $\Delta H$ , and subtract a single concentration-dependent term  $G$ , i.e.,

$$\Delta H(\sigma) = \varepsilon(\sigma) + G(x). \quad (8)$$

The main contribution to  $G(x)$  is the energy needed to change the volumes of the constituents into the equilibrium volume of the compound. This elastic energy is calculated<sup>17</sup> from

$$G(x) = x \int_x^1 (1-y) \frac{B}{V} \left( \frac{dV}{dy} \right)^2 dy + (1-x) \int_0^x y \frac{B}{V} \left( \frac{dV}{dy} \right)^2 dy, \quad (9)$$

where the bulk modulus  $B$ , and the equilibrium volume  $V$ , are both functions of the concentration. A simple way to approximate<sup>17</sup> the elastic energy is to replace Eq. (9) with a form that has the same properties (zero at  $x=0$  and  $x=1$ , and negative second derivative), i.e.,

$$G(x) = \Omega x(1-x). \quad (10)$$

The *effective elastic interaction*  $\Omega$  is defined by the condition that the areas under the two curves are equal.

In systems where the constituents have significantly different volumes, relaxations will be important. A way to deal with this is to do a *mixed-space* CE.<sup>18,19</sup> The long-range pair interactions are handled in reciprocal space. It is well known that a finite CE fails in the long period limit. To reduce the error in the long period limit the reference energy can be chosen as the constituent strain energy,  $\Delta E_{CS}$ .<sup>18</sup> Since the system Re-W has rather small size mismatch, we will in this paper use a real-space CE and use the elastic energy  $G$  in Eq. (10) as the reference energy.

### C. The free energy

In the Helmholtz free energy  $F = E - TS$ , there are several different contributions to the entropy  $S$ , arising from disorder in the atomic configuration, atomic vibrations, and electronic excitations. In the last term, there is an electron-phonon many-body contribution. However, that correction can be neglected when  $T > \theta_D/3$ , where  $\theta_D$  is the Debye temperature.<sup>25</sup>

The configurational part of the entropy is treated with the cluster variation method<sup>20</sup> (CVM). As in the CE it is necessary to introduce some approximation. The fundamental approximation is the assumption that the statistical correlations beyond a largest cluster are negligible. Then the configura-

tional part of the entropy can be written in closed form in terms of the thermodynamical average of the cluster functions, called multisite correlation functions. Having the configurational part of the entropy, we can construct the free energy  $F_{\text{CVM}}$ . This free-energy functional can be minimized using standard techniques.

The vibrational entropy, and therefore the free energy, is not defined for dynamically unstable systems. This problem has a profound impact on thermodynamical calculations of structural free-energy differences.<sup>21–24</sup> We will calculate the phonon frequencies for Re and W in the bcc and fcc structures using the linear response theory. From these results we will estimate the region of dynamical stability for the Re-W system and calculate the vibrational contribution to the free energy in that region. The expression for the vibrational free energy per atom is<sup>25</sup>

$$F_{\text{vibr}}(T) = 3k_{\text{B}}T \int_0^{\infty} g(\nu) \ln \left( 2 \sinh \frac{h\nu}{2k_{\text{B}}T} \right) d\nu. \quad (11)$$

The problem of calculating  $F_{\text{vibr}}$  is thus reduced to finding the phonon density of states (DOS)  $g(\nu)$ . To calculate  $g(\nu)$  we have to obtain the dynamical matrices,  $\mathbf{D}(\mathbf{q})$ , for a large number of  $\mathbf{q}$  points in the first Brillouin zone. For this we employ the general Born–von Kármán model.<sup>26</sup> Assuming that the interaction between the atoms is cut off beyond a distance  $R_{\text{max}}$  we can express the dynamical matrices as

$$\mathbf{D}(\mathbf{q}) = \sum_{|\mathbf{R}| < R_{\text{max}}} e^{-i\mathbf{q} \cdot \mathbf{R}} \mathbf{D}(\mathbf{R}), \quad (12)$$

where  $\mathbf{D}(\mathbf{R})$  are the real-space interatomic force-constant matrices. The usual approach is now to obtain the dynamical matrices from the calculated interatomic or interplanar force constants.<sup>27,28</sup> Here we use the linear response technique to calculate  $\mathbf{D}(\mathbf{q})$  for a small number ( $\sim 30$ ) of  $\mathbf{q}$  points. These matrices are then used in Eq. (12) to extract the real-space force-constants. When the real-space force-constant matrices are determined, Eq. (12) can be used to obtain the  $\mathbf{D}(\mathbf{q})$  for an arbitrary  $\mathbf{q}$ . Hence we are able to calculate  $\nu(\mathbf{q})$  and then  $g(\nu)$ .

To the configurational and the vibrational part of the free energy we add the temperature-dependent part of the electronic free energy,

$$F(T) = F_{\text{CVM}}(T) + F_{\text{vibr}}(T) + F_{\text{el}}(T). \quad (13)$$

The electronic energy  $E_{\text{el}}$  and entropy  $S_{\text{el}}$  are obtained from the density of states,  $D(\epsilon, T)$ , using the expressions for the noninteracting electron gas,

$$E_{\text{el}}(T) = \int_{-\infty}^{\infty} \epsilon D(\epsilon, T) f d\epsilon - \int_{-\infty}^{\epsilon_{\text{F}}} \epsilon D(\epsilon, 0) d\epsilon, \quad (14)$$

$$S_{\text{el}}(T) = -k_{\text{B}} \int_{-\infty}^{\infty} [f(\ln f) + (1-f)\ln(1-f)] D(\epsilon, T) d\epsilon, \quad (15)$$

where  $\epsilon_{\text{F}}$  is the chemical potential  $\mu$ , at zero temperature and  $f$  is the Fermi-Dirac distribution function. When the density of states varies slowly with  $\epsilon$  near the Fermi level,  $D(\epsilon, T)$

can be taken outside the integral as a constant  $D(\epsilon_{\text{F}})$ . We get the Sommerfeld expressions<sup>25</sup> for the electronic energy and entropy and hence

$$F(T) = F_{\text{CVM}}(T) + F_{\text{vibr}}(T) - \frac{\gamma}{2} T^2, \quad (16)$$

where

$$\gamma = \frac{\pi^2}{3} D(\epsilon_{\text{F}}) k_{\text{B}}^2. \quad (17)$$

#### D. Electronic structure and linear response calculations

We used the local density approximation<sup>29</sup> of the density-functional theory.<sup>30</sup> The calculations were performed using a plane-wave basis set and separable norm-conserving pseudopotentials<sup>31</sup> for W and Re with the  $5s$ ,  $5p$ ,  $6s$ ,  $6p$ , and  $5d$  states as valence states. These were generated in the multiple reference energy formalism of Vanderbilt.<sup>32</sup> The core radii were chosen to be 1.8 a.u. for both W and Re and the  $d$  pseudopotential was chosen as the local pseudopotential. This scheme allows a plane-wave energy cutoff of  $E_{\text{cut}} = 40$  Ry and the total energy convergence was better than 0.1 mRy/atom. We used the conjugate gradient method to iteratively solve the Schrödinger equation<sup>33,34</sup> and the modified Broyden mixing scheme<sup>35</sup> to achieve screening self-consistency. The Brillouin zone summations were carried out using the deVita and Gillan finite-temperature method<sup>36</sup> where the electronic occupation numbers are calculated from the Fermi-Dirac distribution. The total-energy calculations were performed at  $T = 290$  K. The total energy at 0 K was obtained from an extrapolation of  $F(T)$  to  $T = 0$  within the Sommerfeld model. We chose a  $16 \times 16 \times 16$  Monkhorst-Pack<sup>37</sup> grid yielding 145  $\mathbf{k}$  points in the irreducible wedge of the Brillouin zone for the bcc and the fcc structure.

The phonon frequencies were calculated using the density-functional linear response method<sup>38</sup> for metallic systems.<sup>39,40</sup> This method is based on the variational principle of the density functional theory as developed by Gonze and Vigneron,<sup>41</sup> which makes it possible to derive the self-consistent equations to all orders of the external perturbation. We obtained an explicit temperature dependence in the phonon frequencies by populating the electron states according to Fermi-Dirac statistics. The calculations were performed at  $T = 570$  K. Several phonon calculations were also performed on a  $20 \times 20 \times 20$  mesh showing that the phonon frequencies were well converged. A cubic spline was used to interpolate between the calculated phonon frequencies to obtain the dispersion curves.

### III. RESULTS

#### A. Total energy calculations

To test the reliability of the pseudopotentials we calculated the lattice constants, bulk moduli, and relative energies for the pure elements in different structures. This was done with the pseudopotentials as well as with a full-potential technique (WIEN-95).<sup>42</sup> The agreement is very good and the results are presented in Table I.

TABLE I. Comparison between pseudopotential and linear-augmented plane-wave (LAPW) results. The energy differences are calculated with the bcc energy as the reference energy.

Composition	Structure	$a_0$ (a.u.)		$B_0$ (GPa)		$\Delta$ (mRy/atom)	
		PW	LAPW	PW	LAPW	PW	LAPW
Re	A1	7.280	7.330	398	404	-18.3	-23.7
Re	A2	5.780	5.837	396	398	0	0
Re	A3	5.159	5.195	401	405	-23.4	-28.3
W	A1	7.480	7.527	305	312	37.4	35.6
W	A2	5.903	5.943	337	335	0	0
W	A3	5.285	5.318	305	308	42.8	41.6

The total energy was then calculated for 10 bcc and 14 fcc superstructures. For illustrative figures see Refs. 16 and 43. The results for the equilibrium lattice constants, bulk moduli, and heats of formation are presented in Tables II and III. All structures were relaxed with respect to external and internal coordinates. The change in total energy was rather small except in three structures. Internal relaxations in Z2 decreased the energy by 4.25 mRy/atom and in Z1 by 3.42 mRy/atom for  $\text{ReW}_3$  and 1.46 mRy/atom for  $\text{Re}_3\text{W}$ . The largest  $c/a$  relaxations were found in Z1( $\text{ReW}_3$ ) where the energy dropped 0.54 mRy/atom. It is interesting to note that both volumes and bulk moduli vary linearly with concentration to a very high accuracy in the Re-W system.

From the total energy calculations for the pure constituents we also obtained the density of states. The coefficient  $\gamma$  in the electronic contribution to the free energy was calculated according to Eq. (17). With the use of the calculated equilibrium volumes and the bulk moduli the effective elastic interaction  $\Omega$  was calculated for the bcc and fcc phase through Eqs. (9) and (10). The results for  $D(\epsilon_F)$  and  $\Omega$  are presented in Table IV. Subtracting the elastic energy  $\Omega x(1-x)$  from the heat of formation yielded the energy that was used to obtain the volume-independent ECI's. To obtain the best fit we calculated the standard deviation,  $\sqrt{w}$ , in Eq. (5) for different sets of interactions for both phases. For the fcc

TABLE II. Structure information for fcc superstructures where  $a_0$  is the lattice parameter,  $B_0$  is the bulk modulus, and  $\Delta^0H$  is the heat of formation.

Composition	Structure	$a_0$ (a.u.)	$B_0$ (GPa)	$-\Delta^0H$ (mRy)
Re	A1	7.280	398	0.00
$\text{Re}_3\text{W}$	$L1_2$	7.324	378	3.58
$\text{Re}_3\text{W}$	$D0_{22}$	7.326	377	2.97
$\text{Re}_3\text{W}$	Z1	7.326	375	3.30
$\text{Re}_2\text{W}$	$\text{MoPt}_2$	7.348	367	3.66
$\text{Re}_2\text{W}_2$	“40”	7.374	353	3.51
$\text{Re}_2\text{W}_2$	Z2	7.337	354	5.82
ReW	$L1_0$	7.373	351	4.40
ReW	$L1_1$	7.372	352	2.51
$\text{ReW}_2$	$\text{MoPt}_2$	7.415	336	4.36
$\text{ReW}_3$	$L1_2$	7.424	332	2.85
$\text{ReW}_3$	$D0_{22}$	7.426	332	2.71
$\text{ReW}_3$	Z1	7.428	330	5.93
W	A1	7.480	305	0.00

CE we needed, in addition to the empty and point interactions, pair interactions up to the fifth neighbor, three three-body interactions, and three four-body interactions to achieve a standard deviation of 0.06 mRy/atom. A largest error of 0.11 mRy/atom was found for  $\text{Re}_3\text{W}$  in the  $D0_{22}$  structure. The bcc CE included the empty and the point clusters, pairs up to the third neighbor, one three-body cluster, and one four-body cluster. This set gave the standard deviation equal to 0.07 mRy/atom. The largest error (0.14 mRy/atom) was for  $\text{Re}_3\text{W}(D0_3)$ .

## B. Phonon dispersion curves

Phonon frequencies in hypothetical bcc or fcc Re have not been calculated before. The elastic constants  $C'$  and  $C_{44}$  for fcc Re have been predicted<sup>44</sup> to be positive, which indicates that fcc Re is metastable. One of the main objectives of this paper is to map out the dynamical and thermodynamical stability of bcc and fcc Re-W alloys. For this we need to estimate the region of dynamical instability of Re in bcc W and W in fcc Re. The stable phase of W has the bcc lattice structure but the fcc structure is dynamically unstable for phonon modes in a large part of the Brillouin zone.<sup>45</sup> Figure 1 shows the calculated phonon dispersion curves for fcc Re at equilibrium volume. We see that all phonon modes in the high-symmetry directions in fcc Re are stable. In particular the long-wavelength  $T_{[1\bar{1}0]}[\xi\xi0]$  and  $T_{[001]}[\xi\xi0]$  modes, corresponding to the elastic constants  $C'$  and  $C_{44}$ , respectively, are stable in agreement with the predictions men-

TABLE III. Structure information for bcc superstructures where  $a_0$  is the lattice parameter,  $B_0$  is the bulk modulus, and  $\Delta^0H$  is the heat of formation.

Composition	Structure	$a_0$ (a.u.)	$B_0$ (GPa)	$-\Delta^0H$ (mRy/atom)
Re	A2	5.784	396	0.00
$\text{Re}_3\text{W}$	$D0_3$	5.812	380	1.78
$\text{Re}_3\text{W}$	$L6_0$	5.812	384	2.37
$\text{Re}_2\text{W}_2$	B11	5.842	365	2.83
$\text{Re}_2\text{W}_2$	B32	5.841	362	1.85
ReW	B2	5.840	364	4.81
ReW	$A_1$	5.841	363	2.55
$\text{ReW}_3$	$D0_3$	5.871	346	2.28
$\text{ReW}_3$	$L6_0$	5.872	345	2.62
W	A2	5.903	337	0.00

TABLE IV. Elastic and electronic information in terms of the effective elastic interaction  $\Omega$  and the density of states at the Fermi level for the different phases.

Lattice	$\Omega$ (mRy/atom)	$D(\epsilon_F)$ (states/atom Ry)	
		Re	W
fcc	8.19	10.4	15.5
bcc	4.64	14.2	5.3
hcp	-	9.5	19.0

tioned above. Three softening anomalies are exhibited. (i) The longitudinal  $[\xi 00]$  mode shows a significant softening around  $\xi=0.6$ . (ii) The  $L[\xi\xi 0]$  mode decreases slightly around  $\xi=0.5$ . (iii) At the zone boundary in the  $[\xi\xi\xi]$  direction the longitudinal branch softens appreciably. These anomalies are also found in NbC and TaC, two well-known superconductors.<sup>40,46</sup> In NbC the anomalies have been explained by large electron-phonon matrix elements for the electron states at the Fermi level.<sup>40</sup> Rhenium-molybdenum alloys in the  $\sigma$  phase and the A15 structure are also superconductors,<sup>6,7</sup> but to our knowledge there has been no study of superconductivity in fcc Re alloys. The similarity between the phonon anomalies found here and those in NbC and TaC suggests a common explanation.

Turning to Fig. 2 we study the phonon dispersion curves of bcc Re, where  $-|\nu|$  is plotted when  $\nu^2(\mathbf{q}) < 0$ . Several instabilities can be observed. (i) There is a pronounced dip around the  $L[\frac{2}{3}\frac{2}{3}\frac{2}{3}]$  mode. This is a manifestation of an instability towards the  $\omega$  phase,<sup>47</sup> which has also been found in  $\beta$ -Zr.<sup>48</sup> (ii) The entire  $T_{[1\bar{1}0]}[\xi\xi 0]$  branch is unstable. The zone-boundary mode of this branch,  $T_{[1\bar{1}0]}[\frac{1}{2}\frac{1}{2}0]$ , has been studied in several systems,<sup>49–52</sup> since it was conjectured that it gives a possible path for the martensitic bcc to hcp transformations. Further, it has been noted that the  $T_{[1\bar{1}0]}[\frac{1}{4}\frac{1}{4}0]$  phonon mode provides a transition path from the bcc to the dhcp structure.<sup>45</sup> The long-wavelength part of the  $T_{[1\bar{1}0]}[\frac{1}{2}\frac{1}{2}0]$  mode corresponds to the elastic constant  $C'$ , which is also negative. These three instabilities result in a completely unstable  $T_{[1\bar{1}0]}[\xi\xi 0]$  branch. We conclude that bcc Re is dynamically unstable for displacements towards

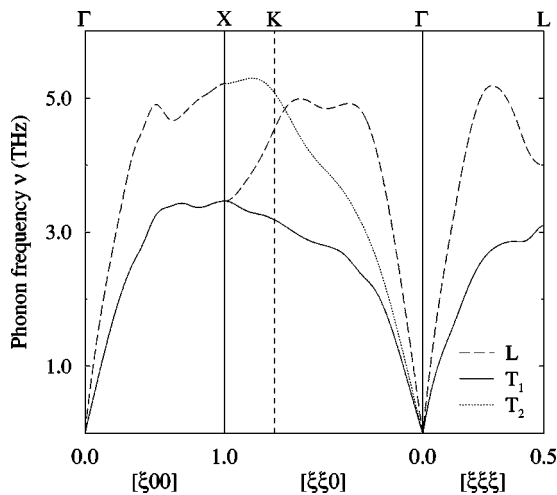


FIG. 1. Calculated phonon frequencies of fcc Re.

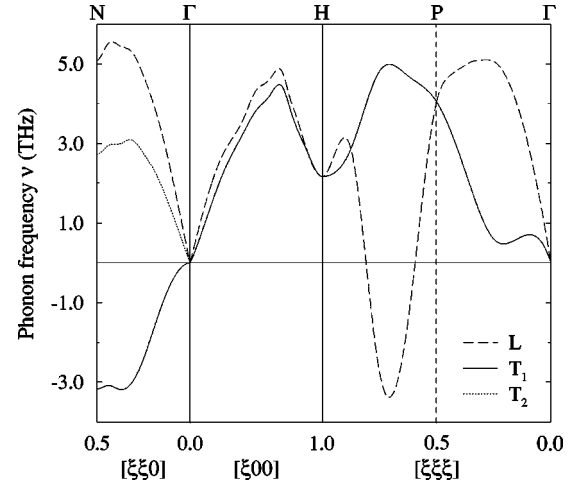


FIG. 2. Calculated phonon frequencies of bcc Re.

the hcp, dhcp, fcc, and  $\omega$  phases. The hcp phase is reached by Burger's path,<sup>53</sup> the dhcp structure through the  $T_{[1\bar{1}0]}[\frac{1}{4}\frac{1}{4}0]$  mode (combined with a shearing of the lattice), the fcc phase through Bain's path, and finally the  $\omega$  phase through the  $L[\frac{2}{3}\frac{2}{3}\frac{2}{3}]$  mode.

### C. Phonon density of states

According to the scheme in Sec. II C we calculated every phonon mode on a  $1.8 \times 10^5$   $\mathbf{q}$  mesh in the irreducible first Brillouin zone for fcc and bcc Re and W. The analysis was performed with interactions extending to the ninth neighbor and seventh neighbor for the fcc and bcc structure, respectively. For the bcc structure only phonons from high-symmetry directions were needed but in the fcc structure an off-symmetry calculation,  $\mathbf{q} = [\frac{1}{8}\frac{3}{4}\frac{3}{4}]$ , was performed to obtain the ninth-neighbor fit. In both fcc Re and fcc W we used forces extending to the eighth-neighbor shell. The W bcc phase was well described with four neighbors but bcc Re needed more long-range forces. A least-squares fit was used to solve for the 19 (29) force-constant matrix elements for the bcc (fcc) structure in 138 (174) linear equations. The model reproduces the dispersion curves for the pure phases very well. Even the anomalies in fcc Re are described accurately. The average deviation in the high-symmetry directions was less than 0.06 THz. From the frequencies we calculated the phonon density of states,  $g(\nu)$ , for the fcc and bcc phases, see Figs. 3 and 4. We normalized  $g(\nu)$  as  $\int_{-\infty}^{\infty} g(\nu) d\nu = 1$ . The bcc W phonon DOS compares well with earlier results<sup>54</sup> and we conclude that fcc Re is indeed a metastable phase because there are no unstable phonon modes anywhere in the Brillouin zone.

To obtain the phonon DOS for the fcc and bcc phases as a function of the concentration we apply the virtual crystal approximation<sup>55</sup> (VCA). We calculate the phonon dispersion curves for a set of different concentrations ( $x=0.25$ ,  $x=0.50$ , and  $x=0.75$ ) in the bcc and fcc structures. From the dynamical matrices we calculate the force constants [Eq. (12)] for the different concentrations in both structures. In other studies, the interatomic force constants have been determined as a function of electron band filling for the transition metals<sup>56</sup> and the phonon dispersion curves for the

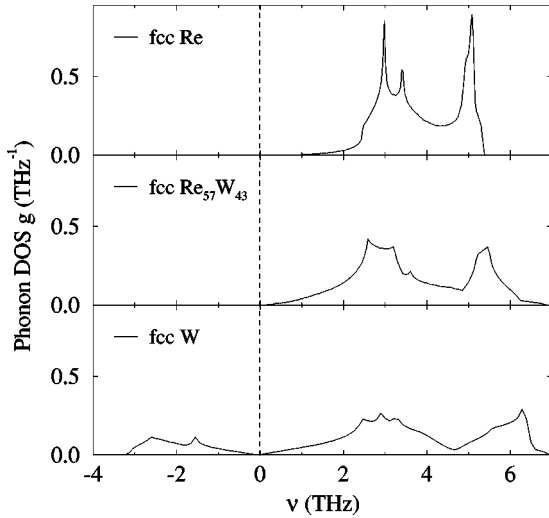


FIG. 3. Calculated phonon DOS of fcc Re,  $\text{Re}_{57}\text{W}_{43}$ , and W.

Nb-Mo system successfully calculated as a function of concentration.<sup>57</sup> Those works<sup>56–58</sup> show that phonon anomalies in transition metals are well described by band filling only. We are interested in integrated quantities such as the vibrational free energy [Eq. (11)] and the vibrational entropy. It is well known that although correct long-range forces are required to model all the features of the phonon dispersion curves, the vibrational entropy converges fast and can be calculated correctly within about 1% with only force constants from the first-neighbor shell.<sup>28</sup> As described in Ref. 58, the force constants in the first-neighbor shells vary smoothly between two neighboring transition elements. Therefore, we interpolate with a cubic spline between the force constants at  $x=0$ ,  $x=0.25$ ,  $x=0.50$ ,  $x=0.75$ , and  $x=1$ , to obtain the phonon DOS and the vibrational free energy for any concentration. In this step we have also used the fact that the masses for W and Re are almost equal, which greatly simplifies the calculation of the phonon DOS in the disordered case. However, the free energy can be obtained in the high-temperature limit even if the atomic masses are not approximately equal. Since the free-energy difference between two competing phases of the same composition is in-

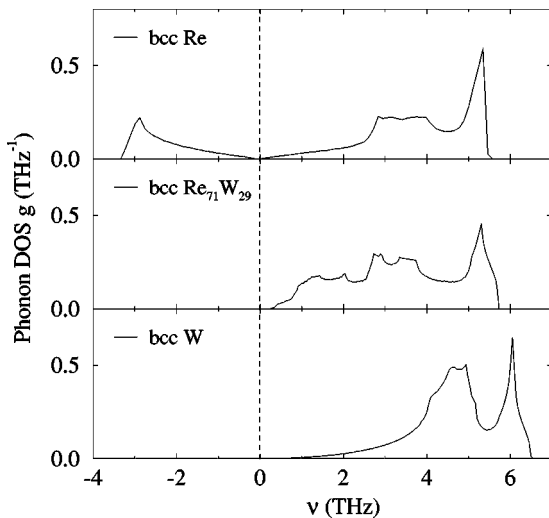


FIG. 4. Calculated phonon DOS of bcc Re,  $\text{Re}_{71}\text{W}_{29}$ , and W.

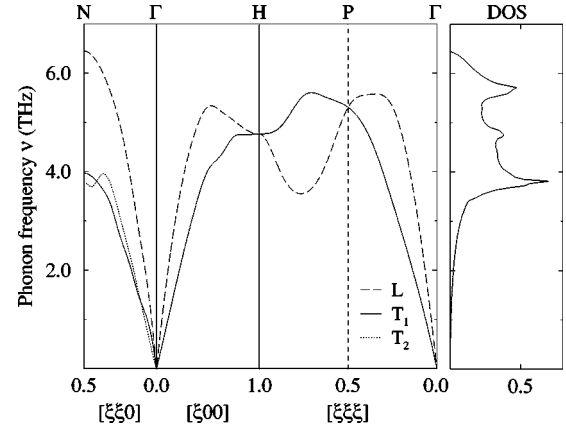


FIG. 5. Calculated phonon frequencies and phonon DOS of bcc  $\text{Re}_{25}\text{W}_{75}$ .

dependent of the atomic masses at high temperatures, it would still be physically correct to interpolate in the force-constant part of the dynamical matrix.<sup>25</sup>

In our model the omega phonon softens first in the bcc structure and the elastic constant  $C'$  softens first in fcc. For the fcc phase we obtain the region of dynamical stability  $0.57 \leq x \leq 1$  and for the bcc phase  $0 \leq x \leq 0.71$ . The central panels in Figs. 3 and 4 display the calculated phonon DOS for the fcc and bcc phases on the verge of instability,  $x=0.57$  and  $x=0.71$ , respectively. By studying the development of the DOS with concentration it is obvious that a part of the intermediate-frequency region has become unstable but that the high-frequency part remains essentially unaltered.

Figure 5 shows the dispersion curves and the phonon DOS for bcc  $\text{Re}_{25}\text{W}_{75}$ , which could be interesting for future neutron-scattering experiments. The dispersion curves are very similar to those of pure bcc W except for a region around the  $H$  point. There is also an incipient softening of the omega phonon.

#### D. The free energy

As an example of how the various terms enter in the free energy we considered our system at  $T=1500$  K. The configurational free energy is minimized with respect to the multisite correlation functions, from which it is possible to calculate the short-range order. At this temperature there is almost no short-range order in the fcc and bcc disordered phase and  $S_{\text{config}}$  is given by  $-k_{\text{B}}x \ln x - k_{\text{B}}(1-x) \ln(1-x)$ . The vibrational free energy is calculated from the phonon DOS for  $0 \leq x \leq 0.71$  in the bcc structure and for  $0.57 \leq x \leq 1$  in the fcc structure, as described in Sec. II C. To add the electronic free energy we calculate  $\gamma$  from Sec. II C as a function of concentration,

$$\gamma(x) = x \gamma_{\text{Re}} + (1-x) \gamma_{\text{W}}. \quad (18)$$

The electronic free energies thus obtained from  $D(\epsilon_{\text{F}})$  were compared with electronic free energies calculated exactly with Eqs. (14) and (15) in the plane-wave code. We conclude that the Sommerfeld approximation of the linear

TABLE V. The different contributions to the free energy at  $T = 1500$  K for bcc W, fcc Re, and for the Re-W system at the instability limits.

Composition (phase)	$F_{\text{config}}$ (Ry/atom)	$F_{\text{vibr}}$ (mRy/atom)	$F_{\text{el}}$ (mRy/atom)
Re(fcc)	-160.3	-60.8	-1.5
Re <sub>57</sub> W <sub>43</sub> (fcc)	-150.5	-63.6	-1.8
Re <sub>71</sub> W <sub>29</sub> (bcc)	-153.9	-66.5	-1.7
W(bcc)	-137.7	-54.7	-0.8

$T$ -dependent entropy works very well for our chosen temperature  $T = 1500$  K and even for higher temperatures ( $T \leq 2000$  K).

The phonon frequencies were calculated at  $T = 570$  K. We also performed a number of calculations at  $T = 1500$  K which showed that the phonon frequencies in W and Re are almost independent of the electronic temperature. Anharmonic effects such as thermal expansion and phonon-phonon interaction are not included in the present calculation. However, thermal expansion is negligible in W (0.4% increase in lattice parameter from 0 K to 1500 K). Rhenium in the hcp structure has a slightly larger linear expansion, 0.8% at 1500 K, so we calculated the phonon dispersion curves for fcc Re at the expanded volume and found only small changes in the phonon frequencies. The explicit anharmonic effects (i.e., beyond the frequency shifts due to thermal expansion) are exceptionally large in bcc W close to the melting temperature.<sup>59</sup> However, the average frequency varies smoothly with  $T$ . At 1500 K, which is much less than the melting temperatures of W (3695 K) and Re (3459 K), we do not expect the explicit anharmonicity to significantly affect the free-energy difference considered here.

In Table V we show the different free-energy contributions to the total free energy at  $T = 1500$  K. Obviously, the difference in the total free energy due to the electronic free energy can be neglected compared to the difference deriving from the configurational and vibrational free energies. The configurational and vibrational free energies are shown as functions of the Re concentration in the upper panel and the total free energy in the lower panel of Fig. 6. All quantities in the figure are calculated as

$$\Delta F_i(x) = F_i(x) - xF_i^{\text{fcc}}(1) - (1-x)F_i^{\text{bcc}}(0), \quad (19)$$

where  $F_i^{\text{fcc}}(1)$  [ $F_i^{\text{bcc}}(0)$ ] represents the configurational, vibrational, and total free energy for Re (W) in the fcc (bcc) structure. From the lower panel in Fig. 6 it is evident that a pure phase separation is not energetically favorable for any concentration compared with the disordered phase. However, as can be seen in the upper panel, if the vibrational free-energy contribution was excluded from the total free energy, a disordered bcc phase would not be energetically favorable in the concentration range  $0.50 \leq x \leq 0.71$  and the fcc phase would hardly be disordered at all. We thus find that the vibrational free-energy contribution significantly influences the thermodynamical properties of the system. Also shown in Fig. 6 is the total free energy for the most favorable of the separated phases where all combinations of the disordered bcc and fcc phases at different concentrations are allowed.

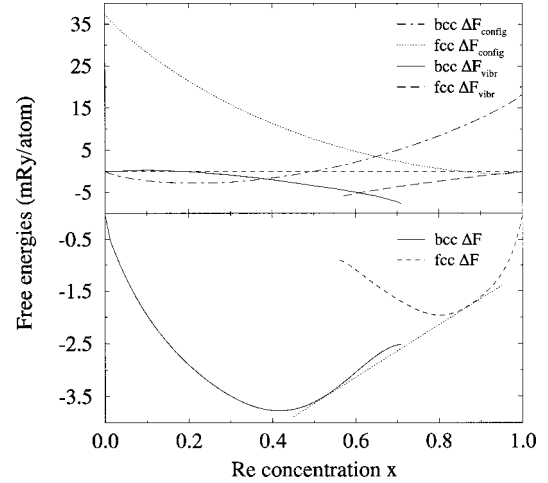


FIG. 6. The upper panel shows the relative configurational and vibrational free energies  $\Delta F$  for bcc and fcc phases as a function of the concentration. The relative total free energy is similarly presented in the lower panel. For the reference energies, see Eq. (21).

This phase decomposition<sup>60</sup> is thermodynamically stable when the tangent construction yields a lower free energy, which in our case occurs for  $0.53 \leq x \leq 0.87$  where a combined disordered bcc and fcc phase is energetically most favorable.

For concentrations slightly higher than  $x = 0.54$ , there is also another possible so-called spinodal decomposition in the bcc phase, where the disordered bcc phase separates into two different disordered bcc phases ( $x = 0.54$  and  $x = 0.71$ ). The formation of the fcc phase requires the system to overcome a nucleation barrier, which means that the spinodal decomposition will be important when the rate of its formation is faster than the kinetics of the nucleation and growth of the more stable bcc-fcc phase combination. Interestingly, if this occurs the disordered bcc phase will transform into a composition ( $x = 0.71$ ) which is on the verge of dynamical instability. As mentioned in Sec. I tungsten is one of the candidate materials for plasma facing components in future nuclear fusion devices and due to the heavy neutron irradiation the Re content may increase from 0 to, say, 25%. If the spinodal decomposition is favorable we note that an aggregation of Re atoms would cause a local martensitic transformation which could have a microstructural effect on the material.

It is interesting to compare the total free energy with its two major contributions displayed in the upper panel. The decrease in vibrational free energy when approaching the instability will extend the stable single-phase region for both the disordered bcc and fcc phases. The thermodynamical stability of the crystal is also enhanced just before the dynamical instability, as an effect of the rapidly decreasing vibrational free energy. This is well illustrated in Ref. 61, where the temperature-pressure ( $T$ - $P$ ) phase diagram of Mg is calculated through a combination of analytic statistical methods and molecular-dynamics simulation. Magnesium has the hcp lattice structure at low  $P$  and the bcc structure at high  $P$ . Below a critical pressure  $P_c$ , the bcc phase is dynamically unstable. Just above  $P = P_c$  the phase diagram shows a slightly increased temperature range where the bcc phase is stable.

#### IV. SUMMARY

We have used *ab initio* total energy and linear response calculations to make a detailed description of the dynamical and thermodynamical stability of the disordered Re-W system. From the dispersion curves for bcc Re we observe that it is dynamically unstable towards the hexagonal, the omega, and the fcc phases. The Re fcc structure is metastable and the phonon dispersion curves exhibit anomalies which can be connected with a strong electron-phonon interaction and therefore suggest superconducting properties. Additional calculations showed that the explicit temperature which enters in the Fermi-Dirac factors and the indirect temperature dependence through thermal expansion introduced only slight changes in the phonon frequencies in Re and W. The force constants and the phonon frequencies in the first Brillouin zone for Re and W in the bcc and fcc phases were obtained through a Born–von Kármán analysis of the dynamical matrices. We present the phonon DOS for the dynamically unstable phases bcc Re and fcc W. For the alloy system we used the virtual crystal approximation to calculate the phonon frequencies. Employing a nonlinear model to the force constants as a function of the concentration we found the stable regions for the disordered bcc and fcc phase. For the stable alloys we were thus able to calculate the vibrational free energy.

In the thermodynamical analysis the different contributions to the free energy have been calculated. We conclude that at  $T = 1500$  K the electronic excitations can be neglected compared to the vibrational and configurational effect on the free-energy differences. We also find that the vibrational free-energy contribution significantly alters the total free energy as a function of the composition and thus influences the thermodynamical as well as the dynamical analysis of the system greatly. Near the dynamical instability the rapidly decreasing vibrational free energy, which is manifested in a small bend in the total free energy, increases the thermodynamical stability of the (metastable) crystal. The phase decomposition for the bcc and fcc phases occurs for Re concentrations, which agrees with the two-phase region in the Re-W phase diagram. A competing spinodal decomposition is also observed which, if important, would cause a second-order transformation.

#### ACKNOWLEDGMENTS

The authors would like to thank V. Ozoliņš for valuable discussions. This work was supported by the Swedish research foundation SSF. The calculations were performed at the Swedish primary national resource for high-performance computing and networking, Paralleldatorcentrum - PDC.

- 
- <sup>1</sup>R. A. Ayres, G. W. Shanette, and D. F. Stein, *J. Appl. Phys.* **46**, 1526 (1975).
- <sup>2</sup>T. Tanabe (private communication).
- <sup>3</sup>K. W. Katahara, M. H. Manghnani, and N. Devnani, *J. Appl. Phys.* **52**, 3360 (1981).
- <sup>4</sup>R. Herschitz and D. N. Seidman, *Acta Metall.* **32**, 1141 (1984); **32**, 1155 (1984).
- <sup>5</sup>*Rhenium and Rhenium Alloys*, edited by B. D. Bryskin (The Minerals, Metals and Materials Society, Warrendale, PA, 1997), pp. 629-728.
- <sup>6</sup>C. C. Koch and J. O. Scarbrough, *Phys. Rev. B* **3**, 742 (1971).
- <sup>7</sup>D. P. Shum, A. Bevolo, J. L. Staudenmann, and E. L. Wolf, *Phys. Rev. Lett.* **57**, 2987 (1986).
- <sup>8</sup>C. W. Chu, W. L. McMillan, and H. L. Luo, *Phys. Rev. B* **3**, 3757 (1971).
- <sup>9</sup>*Binary Alloy Phase Diagrams*, 2nd ed., edited by T. B. Massalski (American Society for Metals, Materials Park, OH, 1990), Vol. 3, p. 3219.
- <sup>10</sup>S. Tournier, B. Vinet, A. Pasturel, I. Ansara, and P. J. Desré, *Phys. Rev. B* **57**, 3340 (1998).
- <sup>11</sup>C. Berne, A. Pasturel, M. Sluiter, and B. Vinet, *Phys. Rev. Lett.* **83**, 1621 (1999).
- <sup>12</sup>L. Cortella, B. Vinet, P. J. Desré, A. Pasturel, A. T. Paxton, and M. van Schilfgaarde, *Phys. Rev. Lett.* **70**, 1469 (1993).
- <sup>13</sup>J. M. Sanchez, F. Ducastelle, and D. Gratias, *Physica A* **128**, 334 (1984).
- <sup>14</sup>J. W. D. Connolly and A. R. Williams, *Phys. Rev. B* **27**, 5169 (1983).
- <sup>15</sup>L. G. Ferreira, S. Wei, and A. Zunger, *Phys. Rev. B* **40**, 3197 (1989).
- <sup>16</sup>Z. W. Lu, S. H. Wei, A. Zunger, S. Frota-Pessoa, and L. G. Ferreira, *Phys. Rev. B* **44**, 512 (1991).
- <sup>17</sup>L. G. Ferreira, A. A. Mbaye, and A. Zunger, *Phys. Rev. B* **37**, 10 547 (1988).
- <sup>18</sup>D. B. Laks, L. G. Ferreira, S. Froyen, and A. Zunger, *Phys. Rev. B* **46**, 12 587 (1992).
- <sup>19</sup>C. Wolverton and A. Zunger, *Phys. Rev. Lett.* **75**, 3162 (1995).
- <sup>20</sup>R. Kikuchi, *Phys. Rev.* **81**, 988 (1951).
- <sup>21</sup>P. J. Craievich and J. M. Sanchez, *Comput. Mater. Sci.* **8**, 92 (1997).
- <sup>22</sup>P. J. Craievich, M. Weinert, J. M. Sanchez, and R. E. Watson, *Phys. Rev. Lett.* **72**, 3076 (1994).
- <sup>23</sup>A. Fernández Guillermet, V. Ozoliņš, G. Grimvall, and M. Körling, *Phys. Rev. B* **51**, 10 364 (1995).
- <sup>24</sup>V. Ozoliņš and A. Zunger, *Phys. Rev. Lett.* **82**, 767 (1999).
- <sup>25</sup>G. Grimvall, *Thermophysical Properties of Materials* (North-Holland, Amsterdam, 1986).
- <sup>26</sup>M. Born and K. Huang, *Dynamical Theory of Crystal Lattices* (Oxford University Press, Oxford, 1985).
- <sup>27</sup>S. Wei and M. Y. Chou, *Phys. Rev. Lett.* **69**, 2799 (1992).
- <sup>28</sup>A. van de Walle, G. Ceder, and U. V. Waghmare, *Phys. Rev. Lett.* **80**, 4911 (1998).
- <sup>29</sup>D. M. Ceperley and B. J. Alder, *Phys. Rev. Lett.* **45**, 566 (1980); J. P. Perdew and A. Zunger, *Phys. Rev. B* **23**, 5048 (1981).
- <sup>30</sup>P. Hohenberg and W. Kohn, *Phys. Rev.* **136**, B864 (1964); W. Kohn and L. J. Sham, *Phys. Rev.* **140**, A1133 (1965).
- <sup>31</sup>B. Sadigh, Ph.D. thesis, Royal Institute of Technology, Sweden, 1997.
- <sup>32</sup>D. Vanderbilt, *Phys. Rev. B* **41**, 7892 (1990).
- <sup>33</sup>M. P. Teter, M. C. Payne, and D. C. Allan, *Phys. Rev. B* **40**, 12 255 (1989).
- <sup>34</sup>D. M. Bylander, L. Kleinman, and S. Lee, *Phys. Rev. B* **42**, 1394 (1990).

- <sup>35</sup>G. P. Srivastava, J. Phys. A **17**, L317 (1984).
- <sup>36</sup>M. J. Gillan, J. Phys.: Condens. Matter **1**, 689 (1989).
- <sup>37</sup>H. J. Monkhorst and J. D. Pack, Phys. Rev. B **13**, 5188 (1976).
- <sup>38</sup>S. Baroni, P. Giannozzi, and A. Testa, Phys. Rev. Lett. **58**, 1861 (1987); P. Giannozzi, S. de Gironcoli, P. Pavone, and S. Baroni, Phys. Rev. B **43**, 7231 (1991).
- <sup>39</sup>V. Ozoliņš, Ph.D. thesis, Royal Institute of Technology, Sweden, 1996.
- <sup>40</sup>S. de Gironcoli, Phys. Rev. B **51**, 6773 (1995).
- <sup>41</sup>X. Gonze and J. P. Vigneron, Phys. Rev. B **39**, 13 120 (1989).
- <sup>42</sup>P. Blaha, K. Schwarz, P. Dufek, and R. Augustyn, WIEN95, Technical University of Vienna, 1995. [Improved and updated Unix version of the original copyrighted WIEN code, which was published in P. Blaha, K. Schwarz, P. Sorantin, and S. B. Trickey, Comput. Phys. Commun. **59**, 399 (1990).]
- <sup>43</sup>M. Asta, D. de Fontaine, M. van Schilfgaarde, M. Sluiter, and M. Methfessel, Phys. Rev. B **46**, 5055 (1992).
- <sup>44</sup>J. M. Wills, O. Eriksson, P. Söderlind, and A. M. Boring, Phys. Rev. Lett. **68**, 2802 (1992).
- <sup>45</sup>K. Einarsson, B. Sadigh, G. Grimvall, and V. Ozoliņš, Phys. Rev. Lett. **79**, 2073 (1997).
- <sup>46</sup>*Dynamical Properties of Solids*, edited by G. K. Horton and A. A. Maradudin (North-Holland, Amsterdam, 1980), Vol. 3, p. 100.
- <sup>47</sup>C. Falter, W. Ludwig, W. Zierau, and M. Selmke, Phys. Lett. **93A**, 298 (1983).
- <sup>48</sup>K.-M. Ho, C.-L. Fu, and B. N. Harmon, Phys. Rev. B **29**, 1575 (1984).
- <sup>49</sup>K.-M. Ho, C.-L. Fu, and B. N. Harmon, Phys. Rev. B **28**, 6687 (1983).
- <sup>50</sup>W. A. Bassett and E. Huang, Science **238**, 780 (1987).
- <sup>51</sup>Y. Chen, K. M. Ho, and B. N. Harmon, Phys. Rev. B **37**, 283 (1988).
- <sup>52</sup>M. Ekman, B. Sadigh, K. Einarsson, and P. Blaha, Phys. Rev. B **58**, 5296 (1998).
- <sup>53</sup>W. G. Burgers, Physica (Amsterdam) **1**, 561 (1934).
- <sup>54</sup>*Phonon States of Elements, Electron States and Fermi Surfaces of Alloys*, edited by K.-H. Hellwege and J. L. Olsen, Landolt-Börnstein New Series, Group III, Vol. 13, Pt. a (Springer-Verlag, Berlin, 1981).
- <sup>55</sup>L. Nordheim, Ann. Phys. (Leipzig) **9**, 607 (1931).
- <sup>56</sup>M. W. Finnis, K. L. Kear, and D. G. Pettifor, Phys. Rev. Lett. **52**, 291 (1982).
- <sup>57</sup>C. M. Varma and W. Weber, Phys. Rev. B **19**, 6142 (1979).
- <sup>58</sup>E. Bruno, B. Ginatempo, E. S. Giuliano, A. V. Ruban, and Yu. Kh. Vekilov, Phys. Rep. **49**, 353 (1994).
- <sup>59</sup>A. Fernández Guillermet and G. Grimvall, Phys. Rev. B **44**, 4332 (1991).
- <sup>60</sup>J. W. Cahn, Acta Metall. **9**, 1368 (1961).
- <sup>61</sup>J. A. Moriarty and J. D. Althoff, Phys. Rev. B **51**, 5609 (1995).